Acta Polytechnica **53**(2):179–184, 2013

available online at http://ctn.cvut.cz/ap/

THE INFLUENCE OF NITROGEN IN Ar+N_2 MIXTURE ON PARAMETERS OF HIGH-TEMPERATURE DEVICE WITH ELECTRIC ARC

Ivana Jakubova[a,*], Josef Senk[b], Ilona Laznickova[b]

[a] *Dept. of Radio Engineering, Faculty of Electrical Engineering and Communication, Brno University of Technology, Brno, Czech Republic*

[b] *Dept. of Power Electrical Engineering, Faculty of Electrical Engineering and Communication, Brno University of Technology, Brno, Czech Republic*

[*] corresponding author: jakubova@feec.vutbr.cz

Abstract. The paper presents the results of numerous experiments carried out on a high temperature device consisting of an arc heater with intensively blasted electric arc and reaction chambers connected to its output. The influence of nitrogen mass concentration (up to 11 %) in working gas Ar+N_2 on voltage–current characteristics, power losses of individual parts and efficiency is studied for two variants of electrical configuration of the device. A short description of the computation of necessary thermodynamic and transport properties of Ar+N_2 mixture is included. The computed properties are then used for evaluation of mean temperature and velocity at certain cross-sections of the device. Conclusions can be useful for the design of high temperature devices operating with argon/nitrogen mixture.

Keywords: arc heater, gas mixture, argon, nitrogen.

1. Introduction

The paper deals with a high-temperature device consisting of an arc heater and reacting chambers connected to its output. The device was designed for laboratory experiments, especially with thermal decomposition of stable environmentally harmful substances. The first part of the device, the arc heater with intensively blasted electric arc serves as a source of heated working gas, which is then mixed up with a decomposed substance in the second part, reacting chambers, where decomposition itself takes place.

The parameters of the device are given both by its geometry, both by working gas used. The influence of some parameters (e.g. channel length, gas flow rate, the sort of working gas) was studied in previous works of the authors [6]. As working medium, mostly pure gas is used to be studied. For instance, Isakaev et al. in [4] deal with the arc heater with segmented stepwise extended anode channel operated on argon. Similarly, the work [6] compares the behavior of an arc heater with pure argon or pure nitrogen. Gas mixtures are studied rarely. According to our previous conclusions, the sort of working gas strongly affects operational parameters of the device which seem to be more beneficial with nitrogen. Unfortunately, reaction with nitrogen may produce toxic compounds. That is why utilization of argon with low admixtures of nitrogen deserves attention.

This work presents the results of numerous experiments carried out on the mentioned high-temperature device with the arc heater operated on argon with up to 11 % of nitrogen. Altogether with the measured data (arc current and voltage, power loss of individual segments of the device, etc.), the computed mean temperatures and velocities of the working medium in significant cross-sections are presented. The aim is to show and judge the influence of concentration of nitrogen on basic operational characteristics of the device with two modified configurations of the anode. Especially the applicable input power, the distribution of power loss along the device, the efficiency, the mean temperature and velocity are compared and conclusions useful for practice are given.

2. Material and Methods

Figure 1 shows the main parts of the device in general. The arc heater includes a copper cathode with a tungsten tip, a cathode shell, an anode channel, and an anode. Electric arc is stabilized by intensive blasting of working gas. Steep decrease of the gas velocity at the anode extension creates suitable conditions for stable attachment of the anode spot there.

The reaction chamber is assembled of three parts; stepwise extension of the first part insures thorough mixing of the working gas with the substance to be decomposed.

The device is designed as a modular structure in order to make it possible to reconfigure all parts of the device and to separately measure parameters of individual segments. Both the arc heater and the reaction chambers are set up of hollow copper rings cooled with water flowing through them. The flow rate and temperature of cooling water are measured to determine power loss of individual segments.

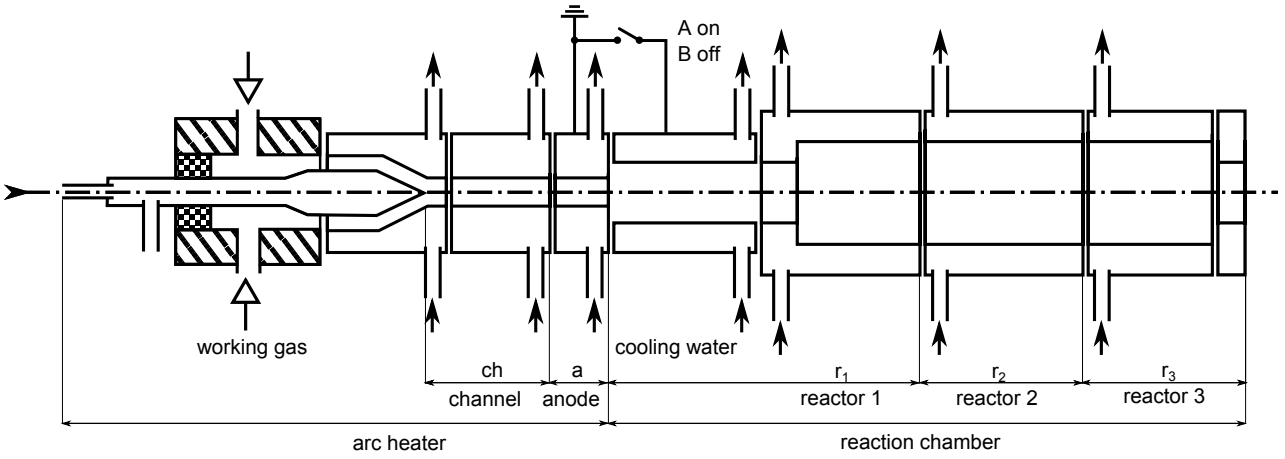

Figure 1. The main parts of the experimental device.

The experiments presented here are focussed on studying the influence of nitrogen mass concentration in argon/nitrogen mixture serving as working gas. That's why other parameters of the device remain unchanged for all the tests: The anode channel is 16 mm in diameter and 109 mm in length. The last section of the anode channel (diameter of 16 mm, length of 27 mm) is always grounded and cooled separately serving as the main anode (referred to as variant B). The first part of the reactor r1 consists of three segments cooled altogether (seg. r11: diameter 30 mm/length 49 mm, electrically isolated, seg. r12: 32 mm/50 mm, seg. r13: 55 mm/30 mm). In one experimental series (referred to as variant A), the first extended part of r11 (34 mm long) is grounded and connected to the last section of the anode channel to improve stability. A decomposed substance is typically added into reactor r1, before its extension from 32 to 55 mm. Thus, in the middle part of the reaction chamber (reactor r2, total length of 92 mm), the working gas and the decomposed substance are perfectly mixed up and reaction conditions (mean temperature and velocity) can be evaluated here. Reactor r3 (89 mm in length) provides additional volume necessary for the technological process and its last segment (25 mm in diameter and 15 mm in length) drains gas away into a scrubber.

The total gas flow rate for the designed device can be set between 2 and 30 $\mathrm{g\,s^{-1}}$. The presented experiments are carried out with the total flow rate of argon/nitrogen mixture of 11.3 $\mathrm{g^{-1}}$. The input power can be up to 60 kW.

The basic set of measured data for each experiment includes arc current, voltage, flow rate of argon and nitrogen, input gas temperature and pressure, and flow rates and temperatures of cooling water in individual segments of the device. The measured voltage U covers not only the arc voltage U_{net} but also the cathode U_{cat} and anode voltage drop U_{an}, thus $U = U_{\mathrm{net}} + U_{\mathrm{cat}} + U_{\mathrm{an}}$. U_{cat} is determined from the measured cathode power loss. For U_{an}, which changes very little with the current, values given in [4] are used.

The cooling water circuits are established according to expected power losses of individual parts of the device and with respect to achievable accuracy. Seven separate water circuits were used (the cathode, cathode shell, anode channel without its last segment, the last anode channel segment, and the first, second and third reactors).

The total power loss of the part of the device from the cathode tip up to the axial distance z_n, i.e. to the n-th output of cooling water, is $P_{\mathrm{l}}(z_n) = \sum_0^n P_{\mathrm{l}i}$. The rest of the input power is transferred to the working medium and results in the increase of its enthalpy; power exchange between the device's outer surface and the surrounding can be neglected. For the arc current I and the cross-section at the distance z_n from the cathode tip, the power P_{h} transferred to the gas is

$$P_{\mathrm{h}}(I, z_n) = UI - P_{\mathrm{l}}(I, z_n). \tag{1}$$

The efficiency of the part of the device up to the cross-section at the distance z_n is

$$\eta(I, z_n) = 1 - \frac{P_{\mathrm{l}}(I, z_n)}{UI}. \tag{2}$$

The practical utilization of the high-temperature device is given especially by attainable parameters of the working medium in the reaction chamber, namely by its temperature and velocity. These quantities can be computed using mass and energy conservation laws. The mean velocity v for the arc current I and distance z_n can be determined using the following relation derived from the continuity equation

$$v(I, z_n) = \frac{4G}{\rho[T(I, z_n)]\pi d^2(z_n)} \tag{3}$$

where ρ is the mass density [$\mathrm{kg\,m^{-3}}$] of the medium, T is the temperature [K], d is the inner diameter [m], all at the distance z_n from the cathode tip, and G is the total gas flow-rate [$\mathrm{kg\,s^{-1}}$].

Similarly, according to the energy equation, the input power covers the power loss of the device, the increase of enthalpy h [J kg^{-1}] and kinetic energy of the heated flowing gas between the beginning $z = 0$ up to the cross-section at the distance z_n from the cathode tip

$$UI = P_l(I, z_n) + G\Delta h[T(I, z_n)] + G\frac{v^2(I, z_n) - v^2(0)}{2}. \quad (4)$$

The mean temperature can be determined from the increase of enthalpy h which is as follows

$$h[T(I, z_n)] - h[T_0] = \frac{P_h(I, z_n)}{G} - \frac{v^2(I, z_n) - v^2(0)}{2}. \quad (5)$$

The second member at the right-hand side of Eqs. 4, 5 can be neglected in approximate estimations. The computation of mean temperatures and velocities is sensible especially in the reaction chamber where the working gas is mixed up and the radial profiles of temperature and velocity are rather flat. The computed mean values of temperature and velocity are sufficient for the description of reaction conditions there. They can be calculated at the output of the anode channel as well, but the centerline temperature and velocity may be much higher here because of presence of a narrow arc column.

As it can be seen from Eqs. 3 to 5, the properties of the working gas must be known for the proper range of temperature and pressure.

For the calculation of the equilibrium composition, the thermodynamic properties (mass density, specific enthalpy, specific heat capacity at constant pressure) and the electrical conductivity, the following 17 species were considered: Ar, N, N_2, N_3, Ar^+, N^+, N^{2+}, N^{3+}, Ar^{2+}, N^{2+}, Ar^{3+}, N^{3+}, Ar^{4+}, N^{4+}, N^{2-}, N^{3-} and e^-. The Ar plasma, N_2 plasma and Ar + N_2 plasma mixture for pressure 1 atm and the temperature range from 300 to 20 000 K were considered. The program Tmdgas [1] and the database TheCoufal [2] were used for the calculation of the composition and the thermodynamic properties. The method of the composition calculation used in Tmdgas is based on the method looking for the minimum of Gibbs free energy. The method of the thermodynamic properties calculation is described in detail in [1]. It requires the knowledge of the values of the chemical potentials of all the system species, the system composition and the composition derivatives. The chemical potentials are determined by the values of the standard enthalpies of formation and the standard thermodynamic functions of the system species. These important values are presented in database TheCoufal [2] containing the data of thermodynamic properties of the individual species created by the elements: C, F, H, N, O, S, W, Ar, Ca, Cl, Cu and e^-.

The method of the transport properties calculation proceeds from the kinetic theory of gases and using the Chapman–Enskog method of the solution

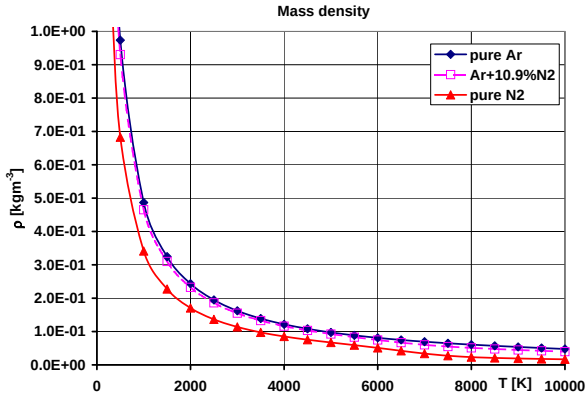

FIGURE 2. Computed mass density of argon, nitrogen, and Ar + 10.9 % of N_2.

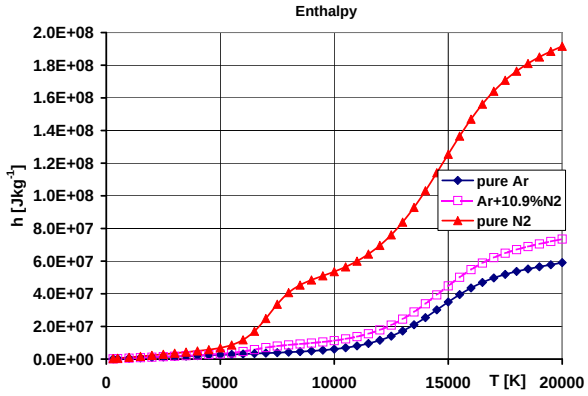

FIGURE 3. Computed enthalpy of argon, nitrogen, and Ar + 10.9 % of N_2.

of the Boltzmann integral–differential equation [3]. The knowledge of the collision integrals of each pair of colliding species in plasma is the integral part of the calculation method. In this paper the fundamental methods of the collision integrals calculation were used; for some pairs of species (e–Ar, e–N, e–N_2, N–N^+, N–N_2) the different methods were applied. Details can be found in [5]. Figures 2 and 3 show the computed mass density and enthalpy for pure argon and nitrogen and for their mixture with mass concentration of 10.9 % of nitrogen.

3. Results and Discussion

In this section, results of selected experiments are given in graphs and discussed. As explained above, the set-up of the device was the same for all the experiments presented here, with anode channel 16 mm in diameter and 109 mm in length. The last segment of the channel was always grounded. For experiments designed "variant A", it was connected to the first extended segment (extended anode 30 mm in diameter and 34 mm in length). The gas flow rate was maintained 11.3 g s^{-1} and the mass concentration was set to 0.6, 1, 1.6, 3, 5, 8, and 10.9 % of nitrogen in the gas mixture. Figure 4 shows the arc voltage U_{net} for both configurations of the device and all the tested mass concentrations of nitrogen in the gas mixture.

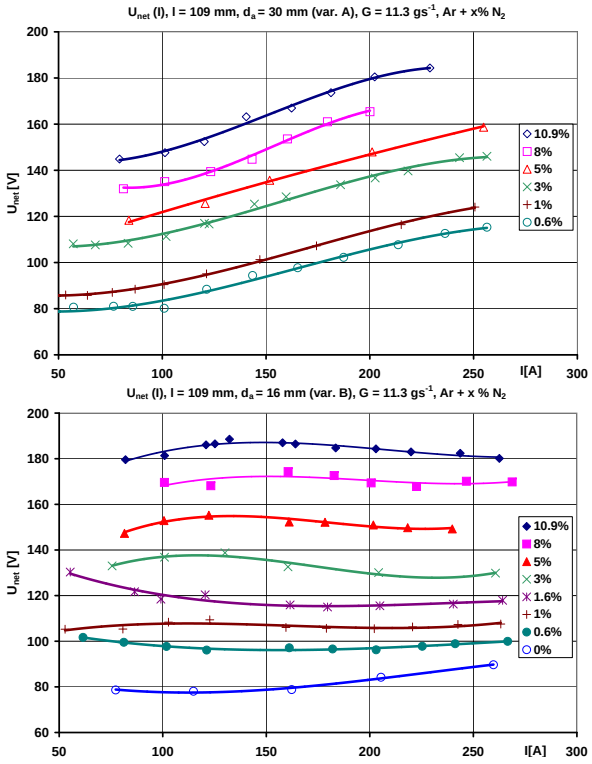

Figure 4. Net arc voltage vs. arc current for various mass concentration of nitrogen in $\mathrm{Ar} + \mathrm{N}_2$ mixture (0 to 10.9 %), total gas flow rate $G = 11.3\ \mathrm{g\,s^{-1}}$, for variant A (anode diameter 30 mm, up) and variant B (16 mm, down).

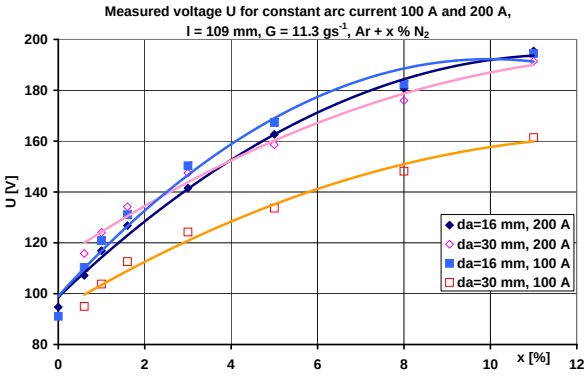

Figure 5. The measured voltage vs. nitrogen mass concentration for both configurations and two currents.

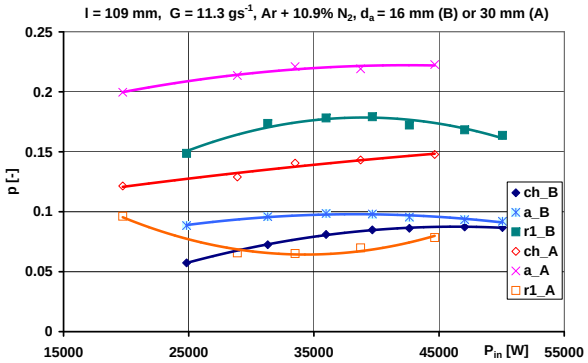

Figure 6. Relative power loss of the selected parts of the device with both configurations (30 mm var. A, 16 mm var. B, ch denotes the anode channel without its last segment, a denotes the anode channel last segment 27 mm in length, r1 is reactor 1), working gas argon with 10.9 % admixture of nitrogen.

For configuration B, also the voltage–current characteristic measured with pure argon is given. Obviously, even a very low mass concentration of nitrogen in the $\mathrm{Ar}+\mathrm{N}_2$ mixture significantly raises the arc voltage. According to Eq. 4 the increase of the arc voltage with the increasing share of nitrogen in the working gas can be explained by higher enthalpy of the mixture (see Fig. 3). While mass density of the mixture with up to 11 % admixture of nitrogen is almost unchanged in comparison to pure argon (see Fig. 2) enthalpy of the mixture is substantially higher. As far as power loss of the anode channel is concerned, measurements for variant A prove it to increase almost linearly with the input power preserving almost the same slope for all the tested concentrations. For the highest tested mass concentration 10.9 %, the arc voltage is more than twice higher than with pure argon.

Comparing the voltage–current characteristics of variant A and B, the arc voltage of the device with the extended anode (variant A) slightly increases in the whole range of the measured currents while the arc voltage of variant B remains almost constant. Thus, operation of the device in variant A exhibits better stability. Because the cathode and anode voltage drops are much lower than the arc voltage as a whole and little sensitive to the current the dependence of the total measured voltage on the current has almost the same shape as $U_{\mathrm{net}}(I)$ (Fig. 4). Consequently, the input power $P_{\mathrm{in}} = UI$ increases almost linearly with the current for variant B, but faster and nonlinearly with the current for variant A (extended anode). From Fig. 5 it can be seen that the voltage increase with the nitrogen mass concentration x slows down for higher concentrations.

Although the total power loss of both configurations is almost the same, surprising distinctions can be revealed if power losses of individual segments are compared. To make comparison easier and more general, the power losses of individual segments are taken relatively to the input power $p_{\mathrm{loss}} = P_{\mathrm{loss}}/P_{\mathrm{in}}$. An example of relative power losses of individual segments of the device operated on argon with 10.9 % admixture of nitrogen and with the both anode configurations is given in Fig. 6. Figure 6 shows the relative power loss of the anode channel without its last segment (ch), of the last anode channel segment (a) and of reactor 1 (r1) for both anode configurations. Relative power losses of other parts of the device are much lower and are not displayed not to make the diagram too complicated. Noticeable differences between both anode configurations can be observed.

In variant A, the relative power loss of the anode channel and its last segment are significantly higher than in variant B and linearly increase with the input

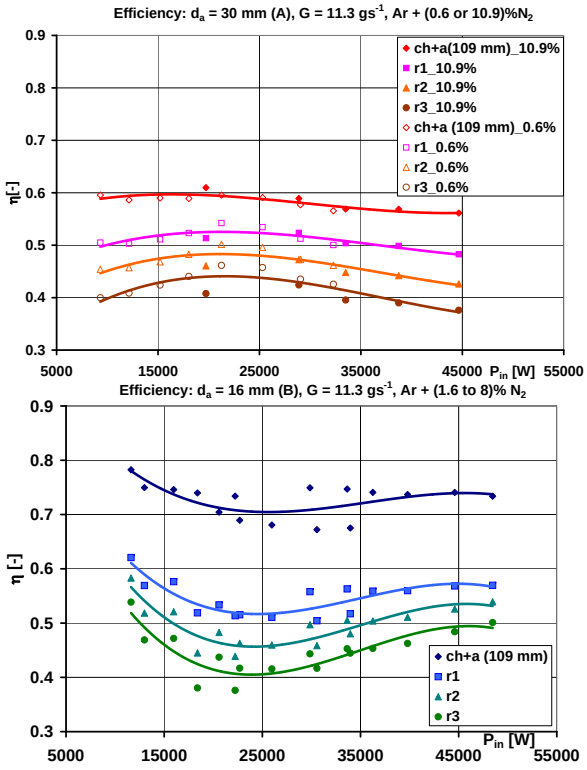

FIGURE 7. Efficiency in important cross-sections of the device, namely at the outputs of the anode channel as a whole (109 mm from the cathode tip) and of the reactors r1, r2, r3 for configuration A (up) and B (down).

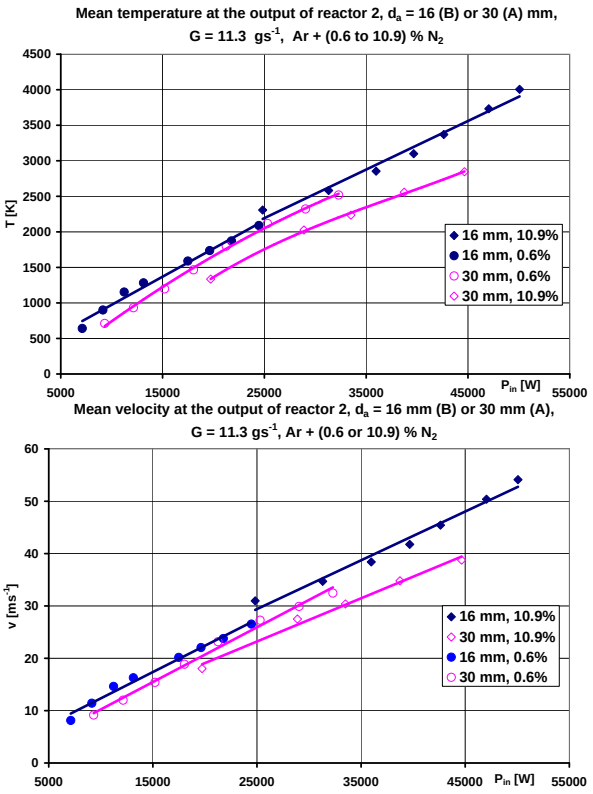

FIGURE 8. Mean temperatures and velocities at the output of reactor 2 for both anode configurations and several nitrogen mass concentrations.

power. On the contrary, the relative power loss of reactor 1 is lower for variant A. The curve of the relative power loss of the first reactor is non-monotonous and exhibits a flat minimum for variant A, but a flat maximum for variant B. For other tested concentrations the power loss distribution is similar.

Figure 7 shows the efficiency in important cross-sections of the device in configuration A and B, namely at the output of the anode channel as a whole (109 mm from the cathode tip) and at the output of each reactor.

Higher mass concentration of nitrogen raises the voltage and consequently higher input power is reached. In Fig. 7 two sets of data are given for configuration A, for the lowest (0.6 %, empty symbols) and the highest (10.9 %, full symbols) tested mass concentrations. Both data sets trace the following parts of the same curve. Similarly, Figure 7 includes the data measured for 1.6 and 8 % for variant B. Comparing the efficiency of the device in both configurations, clearly better efficiency at the output of the anode channel for configuration B compared to configuration A is deteriorated by higher power loss of reactor 1 in variant B. The total efficiency of the device at the output of reactor 3 is between 46 and 37 % for the configuration A ($d_a = 30$ mm) and is slightly lower than in configuration B (52 % to 40 %).

Mean temperatures and velocities were calculated using Eqs. 5 and 3 and the computed enthalpy and mass density of the used $Ar + N_2$ mixtures. As an example, mean temperatures at the output of reactor 2 are depicted in Fig. 8 for both anode configurations and several nitrogen mass concentrations.

Obviously, for configuration B the curve $T(P_{in})$ is almost linear with the same slope for the lowest and highest tested configuration. In configuration A ($d_a = 30$ mm) higher nitrogen mass concentration slightly decreases the mean temperature and the slope of the curve as well. In general, due to higher power loss of the anode channel including its last segment, configuration A exhibits lower mean temperatures than configuration B. Similar conclusions for mean velocities at the output of reactor 2 can be derived from Fig. 8.

4. CONCLUSIONS

Results of experimental operation of the high-temperature device consisting of the arc heater and the three-stage reaction chamber are presented and discussed in the paper. The working gas used was argon with low admixtures of nitrogen (up to approximately 11 %). Two configurations of electrical connection of the anode were tested, with the same geometry of the device.

Even a low admixture of nitrogen in argon was proved to substantially raise the arc voltage under otherwise identical conditions. Thus, the device can

be operated on higher input power. Consequently, the power delivered to the working medium increases as well. It results in higher mean temperatures which can be desirable, and velocities, which can be undesirable. Unfortunately, power loss of the device also increases with the input power. That's why the influence of the increase of nitrogen concentration on the total efficiency is not so simple.

As far as the anode configuration is concerned, variant A with the extended anode $d_a = 30\,\mathrm{mm}$ is characterized by more stable operation. Its voltage–current characteristic is slowly increasing in the tested range and also lower dispersion of measured data proves better stability.

Interesting differences between both anode configurations were observed in power loss distribution along the device. Variant A exhibits substantially bigger power loss of the whole anode channel, including its last grounded segment but surprisingly the power loss of reactor 1 is lower than in variant B. Probably, the arc in configuration A is stabilized in a narrower column in the axis of the anode channel and reaches higher centerline temperature than for variant B. Previous work of the author concluded that it is mainly radiation which transfers energy from the plasma column to the anode channel wall. Thus, both these factors raise radiation and consequently the power loss of the anode channel in variant A compared to variant B.

In the stepwise extended reactor 1, the plasma column is mixed with colder surrounding gas. Smaller radius of the plasma column naturally results in lower mean temperature of the medium in reactor 1 and also lowers power loss of reactor 1 for anode configuration A.

On the contrary, a worse stabilized arc in the anode channel in configuration B (see flat voltage-current characteristics in Fig. 4) probably does not reach too high centerline temperature. Moreover, its lower radiation may be absorbed in outer regions of the wider plasma column. Thus, the power loss of the whole anode channel is lower in variant B, but the mean temperature at its output might be higher than in variant A, which raises the reactor 1 power loss. Obviously, these hypotheses must be tested and confirmed or disproved by further experiments and modeling.

Acknowledgements

The research was performed in Center for Research and Utilization of Renewable Energy Sources. Authors gratefully acknowledge financial support from European Regional Development Fund under project No. CZ.1.05/2.1.00/01.0014.

References

[1] O. Coufal. Composition and thermodynamic properties of thermal plasma up to 50 kK. *Journal of Physics D: Applied Physics* **40**(11):3371–3385, 2007.

[2] O. Coufal, P. Sezemsky, O. Zivny. Database system of thermodynamic properties of individual substances at high temperatures. *Journal of Physics D: Applied Physics* **38**(8):1265–1274, 2005.

[3] J. O. Hirschfelder, Ch. F. Curtis. *Molecular theory of gases and liquids.* John Wiley, New York, 1954.

[4] E.K. Isakaev, et al. Investigation of low temperature plasma generator with divergent channel of the output electrode and some applications of this generator. *High Temperature* **48**(1):97–125, 2010.

[5] I. Laznickova. Transport coefficients of $Ar-N_2$ plasma. In *XIXth Symposium on Physics of Switching Arc*, pp. 271–274. FEKT VUT, Brno, 2011.

[6] J. Senk, I. Jakubova. Properties of a high-temperature device with electric arc burning in various working gas. In *Proceedings of the 13th International Scientific Conference Electric Power Engineering 2012*. BUT FEEC, Brno, 2012.